Research article

Bo Fu[a], Pan Wang[a], Yan Li, Marcello Condorelli, Enza Fazio, Jingxuan Sun, Lijun Xu, Vittorio Scardaci* and Giuseppe Compagnini

Passively Q-switched Yb-doped all-fiber laser based on Ag nanoplates as saturable absorber

https://doi.org/10.1515/nanoph-2020-0015
Received January 10, 2020; revised March 13, 2020; accepted March 16, 2020

Abstract: We report on a Q-switched Yb-doped all-fiber laser based on a solution-processed Ag nanoplates saturable absorber. Optical deposition procedure is implemented to transfer the Ag nanoplates onto the fiber core area through the thermal effect. The saturable absorber is sandwiched between two fiber connectors, providing simplicity, flexibility, and easy integration into the laser oscillator. The modulation depth and saturation incident fluence are measured to be ~5.8% and ~106.36 μJ/cm^2 at 1-μm region, respectively. Self-started stable Q-switched operation is achieved for a threshold pump power of 180 mW. The repetition rates of the pulse trains range from 66.6 to 184.8 kHz when the pump power scales from 210 to 600 mW. The maximum average output power is 10.77 mW, corresponding to the single-pulse energy of 58.3 nJ and minimum pulse duration of ~1.01 μs. To the best of our knowledge, it is the first time that the Ag nanoplates saturable absorbers are utilized in the 1-μm Yb-doped Q-switched fiber laser.

Keywords: Ag nanoplates; saturable absorber; fiber laser; Q-switched.

[a]**Bo Fu and Pan Wang:** These authors contributed equally to this work.
***Corresponding author: Vittorio Scardaci,** Dipartimento di Scienze Chimiche, Università degli Studi di Catania, V.le A. Doria 6, 95125 Catania, Italy, e-mail: vittorio.scardaci@unict.it. https://orcid.org/0000-0003-0167-4368
Bo Fu: BUAA-CCMU Advanced Innovation Center for Big Data-Based Precision Medicine, Interdisciplinary Innovation Institute of Medicine and Engineering, Beijing 100191, P.R. China; and Key Laboratory of Big Data-Based Precision Medicine, Ministry of Industry and Information Technology, School of Medicine and Engineering, Beihang University, Beijing 100191, P.R. China. https://orcid.org/0000-0003-1409-2666
Pan Wang: State key Laboratory of Precision Measurement Technology and Instruments, Department of Precision Instruments, Tsinghua University, Beijing 100084, P.R. China; and Current address: Max Planck Institute for the Science of Light, Staudtstr. 2, 91058, Erlangen, Germany
Yan Li: School of Optoelectronic Engineering, Guangdong Polytechnic Normal University, Guangzhou 510665, P.R. China
Marcello Condorelli and Giuseppe Compagnini: Dipartimento di Scienze Chimiche, Università degli Studi di Catania, V.le A. Doria 6, 95125 Catania, Italy. https://orcid.org/0000-0001-8077-9373 (M. Condorelli)
Enza Fazio: Dipartimento di Scienze Matematiche e Informatiche, Scienze Fisiche e Scienze della Terra, Università di Messina, Messina, Italy
Jingxuan Sun: School of Instrumentation and Optoelectronic Engineering, Beihang University, Beijing 100191, P.R. China
Lijun Xu: BUAA-CCMU Advanced Innovation Center for Big Data-Based Precision Medicine, Interdisciplinary Innovation Institute of Medicine and Engineering, Beijing 100191, P.R. China; and School of Instrumentation and Optoelectronic Engineering, Beihang University, Beijing 100191, P.R. China

1 Introduction

Q-switched laser sources have attracted considerable attention during the past decades due to the versatile applications in widespread industry and scientific research areas, such as laser materials processing, remote sensing, range finding, medicine, telecommunications, and nonlinear optics [1–5]. In Q-switched mechanism, the Q-factor of the cavity is modulated to iteratively induce excited population buildup and abrupt photon emission [6]. The Q-switched laser sources are mainly generating short pulses with pulse duration of micro-second or nano-second level and low repetition rate of kHz. In contrast with the active Q-switched lasers, where costly, complex, and bulky external devices like acoustic- or electro-optic modulators are utilized in the cavity, passively Q-switched lasers with saturable absorbers (SAs) possess the attractive advantages of compactness, simplicity, and flexibility of implementation [7]. In recent years, the investigation of novel high-performance SAs for pulsed laser systems has been a rich and fascinating subject in the field of fiber laser physics, leading to an outburst of publications realized with Q-switched and mode-locked fiber lasers. To date, numerous nanomaterials have been demonstrated as efficient saturable absorption materials for SAs in Q-switched fiber lasers, such as carbon nanotubes [8–10], graphene [11–14], transition-metal dichalcogenides [15–18], topological insulators [19–21], black phosphorus

Open Access. © 2020 Vittorio Scardaci et al., published by De Gruyter. This work is licensed under the Creative Commons Attribution 4.0 Public License.
Published online April 22, 2020

[22–24], quantum dots [25, 26], MXenes [27], filled skutterudites [28], and transition metal oxides [29–31].

Most recently, metal nanoparticles, e.g. gold (Au), silver (Ag), and copper (Cu), have attracted increasing attention due to their distinctively optical and physical properties such as broadband surface plasmon resonance, ultrafast response time, and large third-order nonlinearity [32–35]. The outstanding properties of the metal nanoparticles have been promoting the interesting applications in the areas of optics, medicine, and spectroscopy [36–41]. It is worthy to note that metal nanoparticles have exhibited great potential in the application of ultrafast fiber lasers as SAs for Q-switched and mode-locked pulse generation [42–50]. Up to now, most metal nanoparticles-based SAs researches focus on Au nanoparticles as SAs for achieving Q-switching or mode-locking, implemented in the major fiber lasers (i.e. Yb-, Er-, and Tm-doped fiber lasers) [42–46]. On the other hand, the Ag nanoparticles possess the properties of the highest electrical and thermal conductivities among metal materials, as well as large and ultrafast third-order optical nonlinearities [34, 35, 41], indicating the high potential as SAs in pulsed fiber lasers. Moreover, compared to other materials used as SAs [51–60], Ag nanoparticles are easy to fabricate with no need of purification, and particle size can be controlled. However, despite a few works reported on Ag nanoparticles as SAs for Q-switched pulses generation at 1.5- and 2-μm bands [48–50], the investigation of Ag nanoparticles is still insufficient to date, with no experimental report of Q-switched operation at the 1-μm Yb-doped fiber laser (YDFL). It would be interesting to give more insight into the application of Ag nanoparticles material for SA in the field of ultrafast fiber laser. Plasmon resonance in metal nanoparticles depends on their shape and size. Spherical Ag nanoparticles have their plasmon resonance around 400 nm [61]. Because saturable absorption is a resonant phenomenon, a shape change is needed to red-shift the plasmon resonance to the near infrared (IR) [61].

In this paper, we report on the optical characterization of solution-processed Ag nanoplates and demonstrate their use as SA in YDFL operating at 1-μm band. Stable Q-switched operation is realized, generating the pulse trains with repetition rates ranging from 66.6 to 184.8 kHz when the pump power scales from 210 to 600 mW. To the best of our knowledge, it is the first time that the Ag nanoparticles SA is utilized in the 1-μm Yb-doped Q-switched fiber laser.

2 Fabrication and characterization of Ag nanoplates SA

The Ag nanoplates are fabricated in two steps. Spherical Ag nanoparticles are firstly obtained by chemical reduction of $AgNO_3$ by $NaBH_4$, in the presence of trisodium citrate as stabilizing agent, and secondly converted into flat triangular nanoplates by hydrazine and citrate. The Ag nanoplates feature a plasmon resonance that can be widely tuned across the visible and near-IR range, by simply varying the amount of spherical Ag nanoparticles subjected to transformation into the nanoplates [61]. Figure 1 shows characterization of our Ag nanoplate solution by absorption spectroscopy, scanning electron microscopy (SEM), and open aperture z-scan. Such solution shows a broad plasmon resonance in the 1100–1200 nm region and nanoplate size around 150 nm. Z-scan experiments show transmittance increase from 30% to 50% thus confirming a strong saturable absorption effect. All reagents were sourced from Sigma-Aldrich, Milan, Italy.

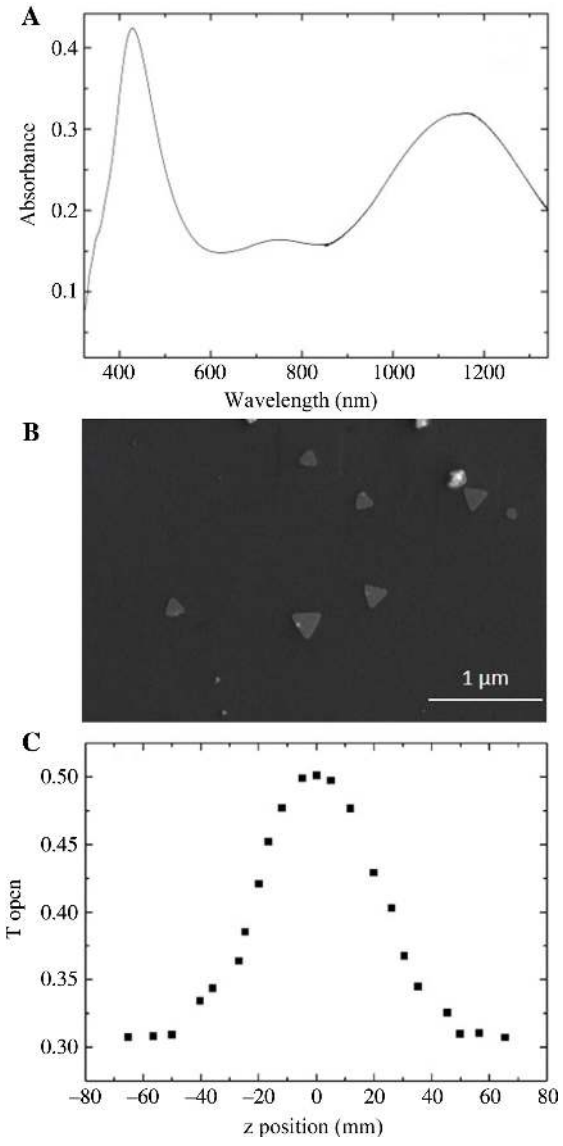

Figure 1: Characterization of the Ag nanoplates solution. (A) Absorption spectrum; (B) SEM image of nanoplates deposited on Si substrate; (C) open aperture Z-scan data.

The Ag nanoplates are deposited on the facet of an optical fiber connector by the extensively reported laser-induced deposition method [48, 62]. As depicted in Figure 2B, the optical deposition procedure is implemented by dipping the distal end of the standard single-mode fiber connector into the solution, under the irradiation of 60 mW continuous wave laser for 30 min, which is generated by a 1550 nm laser source (Santec MLS-8100). As shown in Figure 2D, the Ag nanoplates are deposited by thermal effect and attached to the fiber core area, enabling the interaction with the light propagating in the fiber. Finally, the Ag nanoplates SA is self-assembled by fixation of the two fiber connectors, as illustrated in Figure 3.

The nonlinear saturable absorption property of the Ag nanoplates SA is investigated by measuring the power-dependent transmission based on a twin-detector measurement technique [63].

The experiment is implemented with a home-made 1-μm mode-locked fiber laser source, depicted in Figure 4. An Yb-doped dissipative soliton oscillator serves as the seed laser, and the nonlinear polarization rotation technique is utilized for mode-locking, generating pulse train with repetition rate of 64.2 MHz and pulse duration of ~4.2 ps. After amplification by a two-stage Yb-doped fiber amplifier (YDFA) and compression by a pair of gratings with 1000 lines/mm, the average output power of the pulse train is scaled beyond 300 mW, with pulse duration of ~540 fs, shown in Figure 5B.

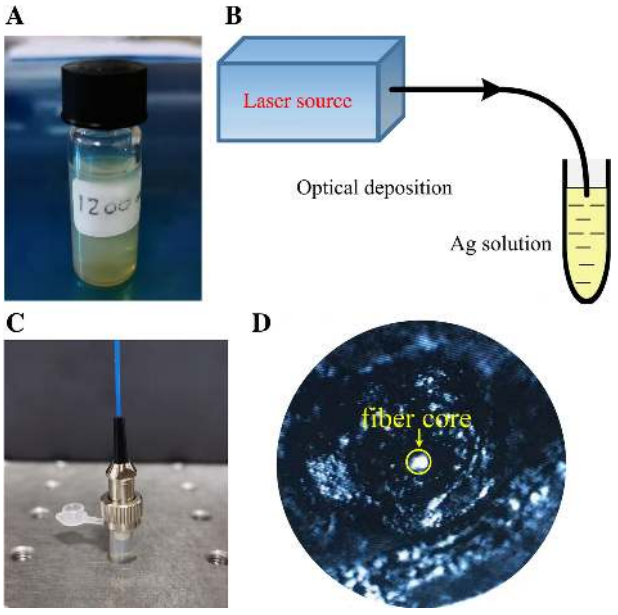

Figure 2: Optical deposition of Ag nanoplates.
(A) The solution with ~150 nm wide Ag nanoplates prepared, resulting in a plasmon resonance at ~1200 nm; (B) scheme of laser-induced deposition method; (C) image of optical deposition to induce the Ag nanoplates to fiber facet; (D) fiber facet with Ag nanoplates after optical deposition.

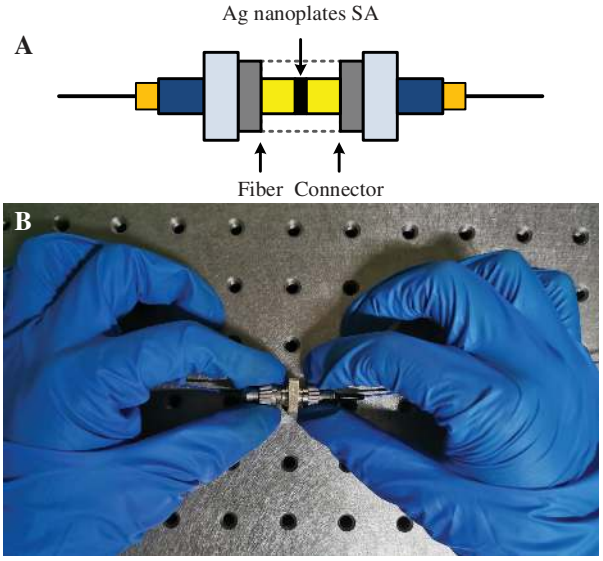

Figure 3: Self-assembly conducted Ag nanoplates SA.

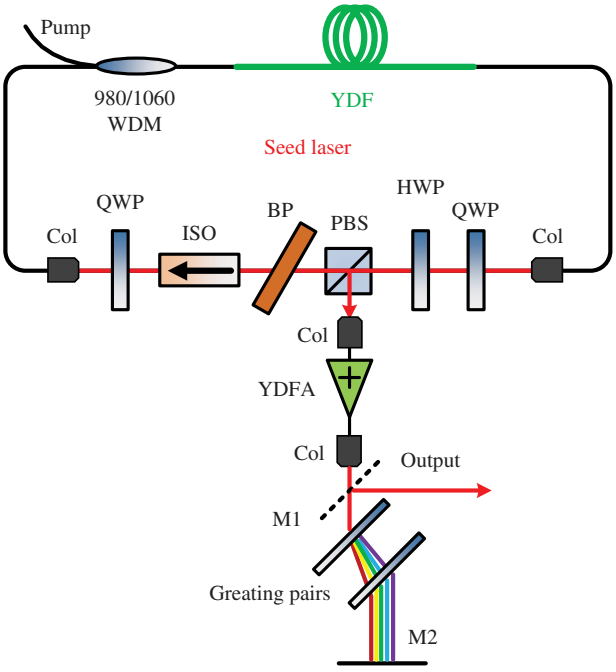

Figure 4: Home-made 1-μm mode-locked fiber laser for the measurement of nonlinear saturable absorption property of the Ag nanoplates SA.
Col, collimator; WDM, wavelength division multiplexer; YDF, Yb-doped fiber; HWP, half wave plate; QWP, quarter wave plate; PBS, polarization beam splitter; BP, birefringent plate; YDFA, Yb-doped fiber amplifier; ISO, isolator; M, mirror.

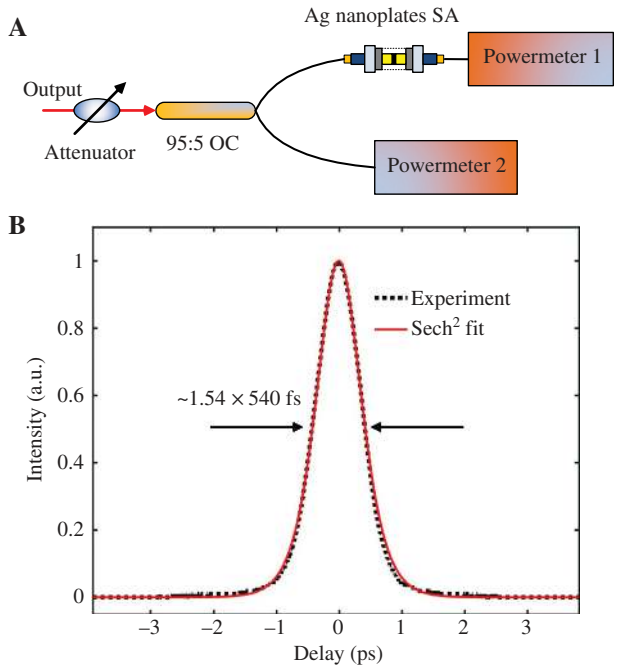

Figure 5: Experimental setup for the measurement of nonlinear saturable absorption property.
(A) Schematic experimental setup for measurement of the nonlinear saturable absorption property of the Ag nanoplates SA. (B) Optical autocorrelation trace of the pulse train for the measurement.

The configuration to characterize the nonlinear saturable absorption property is schematically shown in Figure 5A. The output of the home-made 1-μm mode-locked fiber laser source is modulated by a variable optical attenuator and divided by a 95:5 optical coupler. Ninety-five percent of the power passes through the Ag nanoplates SA and is measured by a power meter, while the other 5% is monitored by another reference power meter. The nonlinear transmittance of the Ag nanoplates SA is shown in Figure 6, as a function of the incident fluence. Fitted with the saturable absorption formula [27], the saturation incident fluence and the modulation depth are estimated to be ~106.36 μJ/cm² and ~5.8%, respectively.

3 Experimental setup and results

The schematic construction of the Q-switched YDFL is illustrated in Figure 7. A piece of ~1.8 m moderately Yb-doped fiber (YDF, Nufern SM-YSF-LO, 80 dB/km core absorption at 980 nm, the dispersion is –37 ps/nm/km at 1060 nm) serves as the gain medium and is backward pumped by a 980 nm laser diode through a 980/1060 nm wavelength division multiplexer (WDM). A polarization-insensitive isolator (PI-ISO) is utilized to provide unidirectional operation. Two polarization controllers (PCs), as well as an 8-nm band pass filter centered at 1030 nm, are employed to optimize the Q-switching pulse operation. The rest of the cavity is composed of ~17.7 m standard single-mode fibers, yielding a total cavity length of ~19.5 m. A 20/80 optical coupler is used to extract 20% of the generated laser for measurement.

The output is monitored by an optical spectrum analyzer (Agilent 86142B) with 0.06-nm resolution, a 1-GHz photodetector recorded by a 2-GHz oscilloscope (Agilent Infiniium DSO80204B), and a radio frequency (RF) signal analyzer (Agilent N9020A).

In our experiment, continuous wave lasing is obtained at the pump power of 130 mW. With appropriate PC settings, stable passive Q-switching is self-started by further increasing the pump power to a certain threshold value of 180 mW.

Figure 8 shows the typical Q-switching characteristics of the YDFL at the pump power of 300 mW. As shown in Figure 8A, the central wavelength of the Q-switched

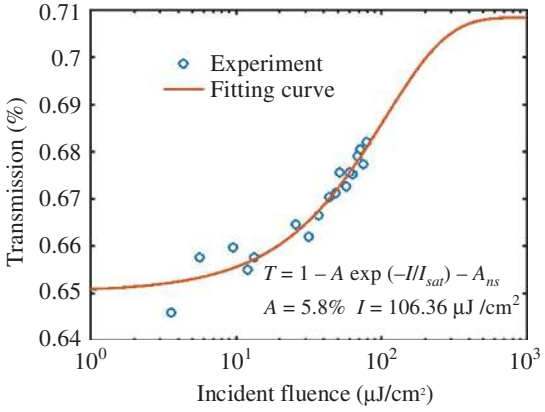

Figure 6: Nonlinear transmittance as a function of incident fluence.

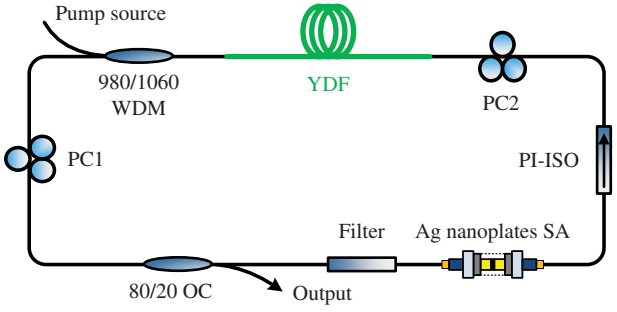

Figure 7: Scheme of the Q-switched Yb-doped fiber laser.
WDM, wavelength division multiplexer; YDF, Yb-doped fiber; PC, polarization controller; PI-ISO, polarization-insensitive isolator; Filter, 1-μm band pass filter; OC, optical coupler.

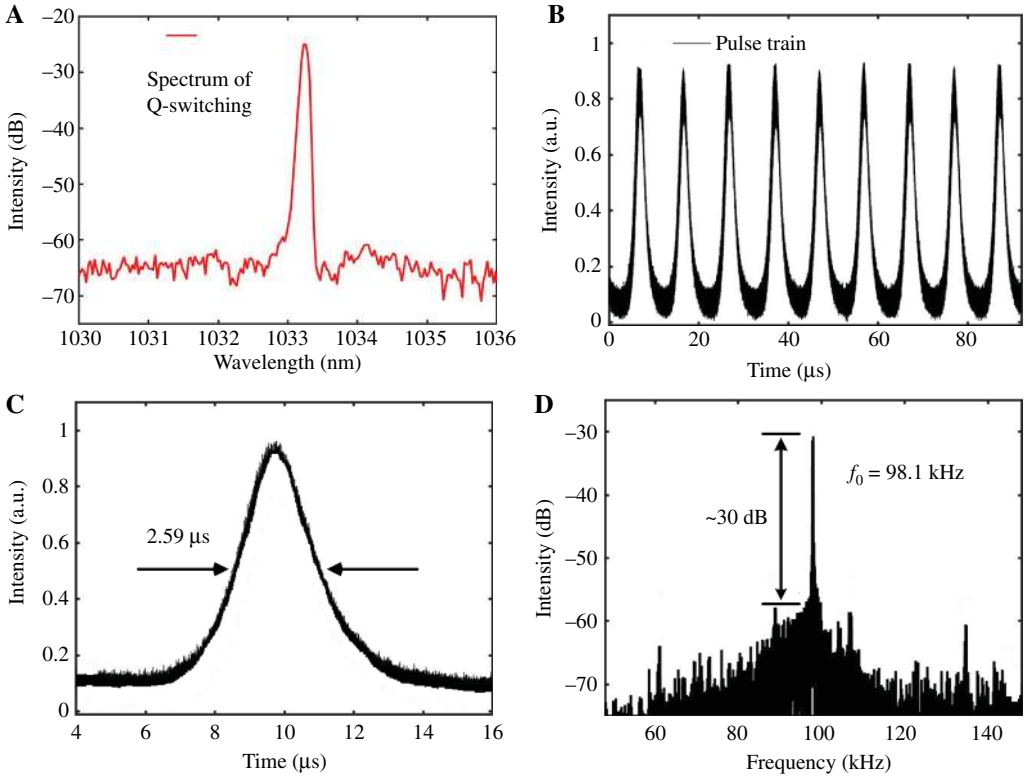

Figure 8: Stable Q-switched operation at the pump power of 300 mW.
(A) Optical spectrum; (B) temporal sequences of output pulse recordings; (C) single-pulse profile of the Q-switched pulse train; (D) RF spectrum over a 100 kHz span with resolution bandwidth of 10 Hz.

operation locates around 1033.3 nm with 3-dB spectral bandwidth of 0.24 nm. Figure 8B shows the temporal waveform of the pulse train on the oscillator, with a 10.19-μs period. The single-pulse profile of the Q-switched pulse train is presented in Figure 8C in a symmetrical Gaussian-like shape. The full width at half-maximum of the pulse profile is measured to be ~2.59 μs, which is the typical time scale of Q-switched operation. The RF spectrum is also measured (Figure 8D) with a repetition rate of 98.1 kHz and more than 30-dB signal-to-noise ratio, confirming relatively stable operation. The long-term stability is also investigated by measuring the output power as well as the repetition rate as a function of time for hours as shown in Figure 9, indicating the stable operation of the laser.

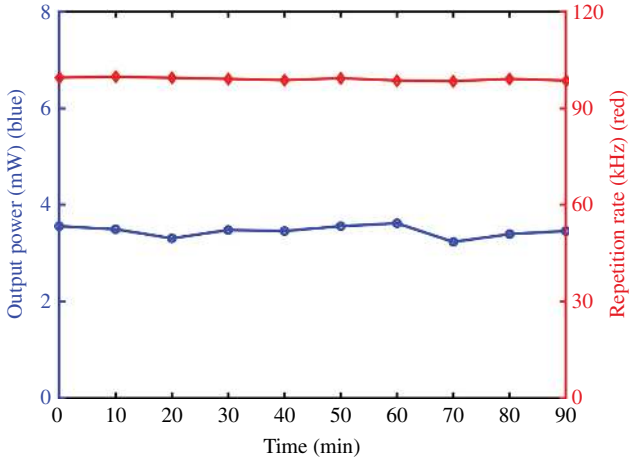

Figure 9: Measurements of output power and pulse repetition rate for long-term stability.

The pulse repetition rate, pulse duration, output power, and pulse energy versus the pump power are further measured, as shown in Figures 10 and 11. In contrast with the repetition rate of mode-locked operation, which is determined by the cavity length, the repetition rate of Q-switched pulses is dependent on the pump power. Attributed to the dependence of Q-switched pulse generation on the saturation of the SA, higher pump power provides much more gain to saturate the SA within a shorter time, which leads to faster bleaching of the Ag nanoplates SA, resulting in the increase of the repetition rate. As shown in Figure 10, in our experiment, the pulse repetition rate of the Q-switched operation increases

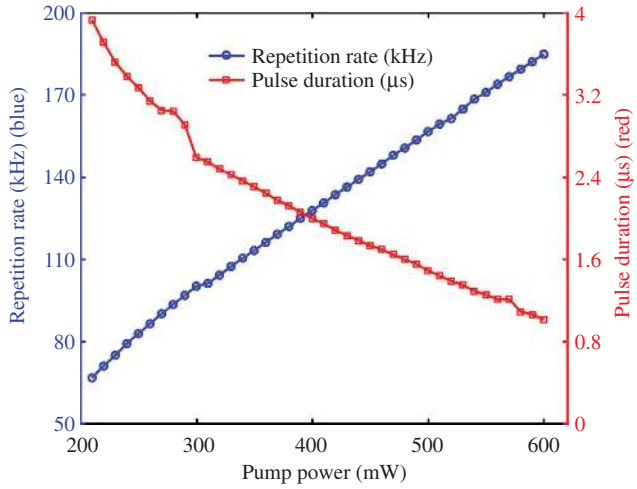

Figure 10: Pulse repetition rate and pulse duration versus the pump power.

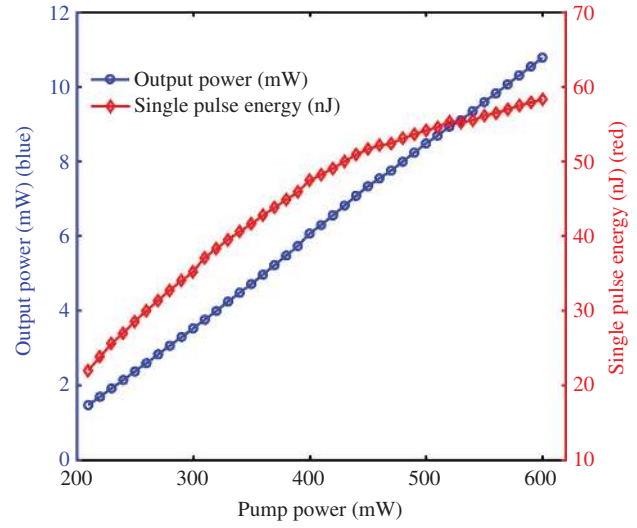

Figure 11: Output power and single-pulse energy vary with the increasing pump power.

monotonically with the increase of the pump power. The pulse repetition rate changes from 66.6 to 184.8 kHz, and the pulse duration decreases from ~3.93 to ~1.01 μs, when the pump power scales from 210 to 600 mW.

The output power and single-pulse energy as a function of pump power are presented in Figure 11. By increasing the pump power from 210 to 600 mW, the output power varies from 1.46 to 10.77 mW, and the single-pulse energy changes from 21.9 to 58.3 nJ. At the pump power of 600 mW, the maximum average output power is 10.77 mW for 184.8 kHz repetition rate, corresponding to the single-pulse energy of 58.3 nJ. The maximum average output power of the pulse train is limited by the pump source in our experiments. The stability of the laser and the maximum pulse energy can be further improved by optimizing the design of the Ag nanoplates SA as well as the structure of the laser cavity.

4 Conclusions

We experimentally investigate Ag nanoplates as SA for Q-switched pulse generation in YDFL. The stable self-started Q-switched operation is achieved for a threshold pump power of 180 mW. The pulse train repetition rate increases with the increase of the pump power. At the maximum pump power of 600 mW, the maximum repetition rate and average output power are 184.8 kHz and 10.77 mW, respectively, corresponding to single-pulse energy of 58.3 nJ. To the best of our knowledge, it is the first demonstration of the passively Q-switched fiber laser by using Ag nanoparticles at the wavelength of 1-μm region. Our results demonstrate the flexibility of the solution-processed Ag nanoplates as SAs, making it a promising candidate for achieving a variety of stable and low-cost ultrafast lasers.

Funding: This work was supported by Beijing Natural Science Foundation (4202044), National Key Research and Development Project (2018YFB2003200), National Natural Science Foundation of China (61827802 and 61961130393), Fundamental Research Funds for the Central Universities, and Open Fund of IPOC (BUPT). The work was also supported by Ministero della Università e della Ricerca-MIUR-(Project ARS01_00519-BEST4U). The authors also acknowledge Fondi di ateneo 2020-2022, Università di Catania, linea Open Access.

References

[1] Stuart BC, Feit MD, Rubenchik AM, Shore BW, Perry MD. Laser-induced damage in dielectrics with nanosecond to subpicosecond pulses. Phys Rev Lett 1995;74:2248–51.
[2] Xu D, Wang Y, Li H, Yao J, Tsang YH. 104 W high stability green laser generation by using diode laser pumped intracavity frequency-doubling Q-switched composite ceramic Nd: YAG laser. Opt Express 2007;15:3991–7.
[3] McGrath AJ, Munch J, Smith G, Veitch P. Injection-seeded, single-frequency, Q-switched erbium: glass laser for remote sensing. Appl Opt 1998;37:5706–9.
[4] Skorczakowski M, Swiderski J, Pichola W, et al. Mid-infrared Q-switched Er:YAG laser for medical applications. Laser Phys Lett 2010;7:498–504.
[5] Shi W, Leigh M, Zong J, Jiang S. Single-frequency terahertz source pumped by Q-switched fiber lasers based on difference-frequency generation in GaSe crystal. Opt Lett 2007;32:949–51.

[6] Paschotta R, Häring R, Gini E, et al. Passively Q-switched 0.1-mJ fiber laser system at 1.53 μm. Opt Lett 1999;24:388–90.
[7] Keller U. Recent developments in compact ultrafast lasers. Nature 2003;424:831–8.
[8] Zhou DP, Wei L, Dong B, Liu WK. Tunable passively Q-switched erbium-doped fiber laser with carbon nanotubes as a saturable absorber. IEEE Photonics Technol Lett 2009;22:9–11.
[9] Kasim N, Al-Masoodi AHH, Ahmad F, Munajat Y, Ahmad H, Harun SW. Q-switched ytterbium doped fiber laser using multi-walled carbon nanotubes saturable absorber. Chin Opt Lett 2014;12:031403.
[10] Chernysheva M, Mou C, Arif R, et al. High power Q-switched thulium doped fibre laser using carbon nanotube polymer composite saturable absorber. Sci Rep 2016;6:24220.
[11] Luo Z, Zhou M, Weng J, et al. Graphene-based passively Q-switched dual-wavelength erbium-doped fiber laser. Opt Lett 2010;35:3709–11.
[12] Popa D, Sun Z, Hasan T, Torrisi F, Wang F, Ferrari AC. Graphene Q-switched, tunable fiber laser. Appl Phys Lett 2011;98:073106.
[13] Liu J, Wu S, Yang QH, Wang P. Stable nanosecond pulse generation from a graphene-based passively Q-switched Yb-doped fiber laser. Opt Lett 2011;36:4008–10.
[14] Tang Y, Yu X, Li X, Yan Z, Wang Q. High-power thulium fiber laser Q switched with single-layer graphene. Opt Lett 2014;39:614–7.
[15] Luo Z, Huang Y, Zhong M, et al. 1-, 1.5-, and 2-μm fiber lasers Q-switched by a broadband few-layer MoS_2 saturable absorber. J Lightwave Technol 2014;32:4077–84.
[16] Woodward RI, Howe RCT, Runcorn TH, et al. Wideband saturable absorption in few-layer molybdenum diselenide ($MoSe_2$) for Q-switching Yb-, Er- and Tm-doped fiber lasers. Opt Express 2015;23:20051–61.
[17] Chen B, Zhang X, Wu K, Wang H, Wang J, Chen J. Q-switched fiber laser based on transition metal dichalcogenides MoS_2, $MoSe_2$, WS_2, and WSe_2. Opt Express 2015;23:26723–37.
[18] Wang X, Cheng PK, Tang CY, et al. Laser Q-switching with PtS_2 microflakes saturable absorber. Opt Express 2018;26:13055–60.
[19] Chen Y, Zhao C, Chen S, et al. Large energy, wavelength widely tunable, topological insulator Q-switched erbium-doped fiber laser. J Sel Top Quantum Electron 2013;20:315–22.
[20] Luo Z, Huang Y, Weng J, et al. 1.06 μm Q-switched ytterbium-doped fiber laser using few-layer topological insulator Bi_2Se_3 as a saturable absorber. Opt Express 2013;21:29516–22.
[21] Luo Z, Liu C, Huang Y, et al. Topological-insulator passively Q-switched double-clad fiber laser at 2 μm wavelength. J Sel Top Quantum Electron 2014;20:1–8.
[22] Chen Y, Jiang G, Chen S, et al. Mechanically exfoliated black phosphorus as a new saturable absorber for both Q-switching and mode-locking laser operation. Opt Express 2015;23:12823–33.
[23] Chu Z, Liu J, Guo Z, Zhang H. 2 μm passively Q-switched laser based on black phosphorus. Opt Mater Express 2016;6:2374–9.
[24] Wang J, Xing Y, Chen L, et al. Passively Q-switched Yb-doped all-fiber laser with a black phosphorus saturable absorber. J Lightwave Technol 2018;36:2010–6.
[25] Lee YW, Chen CM, Huang CW, Chen SK, Jiang JR. Passively Q-switched Er^{3+}-doped fiber lasers using colloidal PbS quantum dot saturable absorber. Opt Express 2016;24:10675–81.
[26] Hisyam MB, Rusdi MF, Latiff AA, Harun SW. PMMA-doped CdSe quantum dots as saturable absorber in a Q-switched all-fiber laser. Chin Opt Lett 2016;14:081404.
[27] Lee J, Kwon S, Lee JH. Ti_2AlC-based saturable absorber for passive Q-switching of a fiber laser. Opt Mater Express 2019;9:2057–66.
[28] Lee J, Yu BK, Jhon YI, et al. Filled skutterudites for broadband saturable absorbers. Adv Opt Mater 2017;5:1700096.
[29] Ahmad H, Lee CSJ, Ismail MA, et al. Tunable Q-switched fiber laser using zinc oxide nanoparticles as a saturable absorber. Appl Opt 2016;55:4277–81.
[30] Bai X, Mou C, Xu L, Wang S, Pu S, Zeng X. Passively Q-switched erbium-doped fiber laser using Fe_3O_4-nanoparticle saturable absorber. Appl Phys Express 2016;9:042701.
[31] Al-hayali SKM, Mohammed DZ, Khaleel WA, Al-janabi AH. Aluminum oxide nanoparticles as saturable absorber for C-band passively Q-switched fiber laser. Appl Opt 2017;56:4720–6.
[32] Liao HB, Xiao RF, Fu JS, Yu P, Wong GKL, Sheng P. Large third-order optical nonlinearity in Au: SiO_2 composite films near the percolation threshold. Appl Phys Lett 1997;70:1–3.
[33] Varnavski OP, Goodson III T, Mohamed MB, El-Sayed MA. Femtosecond excitation dynamics in gold nanospheres and nanorods. Phys Rev B 2005;72:235405.
[34] Chen F, Cheng J, Dai S, et al. Third-order optical nonlinearity at 800 and 1300 nm in bismuthate glasses doped with silver nanoparticles. Opt Express 2014;22:13438–47.
[35] Singh V, Aghamkar P. Surface plasmon enhanced third-order optical nonlinearity of Ag nanocomposite film. Appl Phys Lett 2014;104:111112.
[36] Huang X, Qian W, El-Sayed IH, El-Sayed MA. The potential use of the enhanced nonlinear properties of gold nanospheres in photothermal cancer therapy. Lasers Surgery Med 2007;39:747–53.
[37] De M, Ghosh PS, Rotello VM. Applications of nanoparticles in biology. Adv Mater 2008;20:4225–41.
[38] Kim KH, Husakou A, Herrmann J. Saturable absorption in composites doped with metal nanoparticles. Opt Express 2010;18:21918–25.
[39] Zhang Y, Hu X, Yang H, Gong Q. Multi-component nanocomposite for all-optical switching applications. Appl Phys Lett 2011;99:141113.
[40] Chaudhuri RG, Paria S. Core/shell nanoparticles: classes, properties, synthesis mechanisms, characterization, and applications. Chem Rev 2011;112:2373–433.
[41] Krutyakov YA, Kudrinskiy AA, Olenin AY, Lisichkin GV. Synthesis and properties of silver nanoparticles: advances and prospects. Russ Chem Rev 2008;77:233–57.
[42] Jiang T, Kang Z, Qin G, Zhou J, Qin W. Low mode-locking threshold induced by surface plasmon field enhancement of gold nanoparticles. Opt Express 2013;21:27992–8000.
[43] Kang Z, Guo X, Jia Z, et al. Gold nanorods as saturable absorbers for all fiber passively Q-switched erbium-doped fiber laser. Opt Mater Express 2013;3:1986–91.
[44] Kang Z, Liu MY, Gao XJ, et al. Mode-locked thulium-doped fiber laser at 1982 nm by using a gold nanorods saturable absorber. Laser Phys Lett 2015;12:045105.
[45] Wu H, Song J, Wu J, et al. Concave gold bipyramid saturable absorber based 1018 nm passively Q-switched fiber laser. J Sel Top Quantum Electron 2018;24:0901206.

[46] Muhammad AR, Zakaria R, Ahmad MT, Wang P, Harun SW. Pure gold saturable absorber for generating Q-switching pulses at 2 μm in thulium-doped fiber laser cavity. Opt Fiber Technol 2019;50:23–30.
[47] Muhammad AR, Ahmad MT, Zakaria R, et al. Q-switching pulse operation in 1.5-μm region using copper nanoparticles as saturable absorber. Chin Phys Lett 2017;34:034205.
[48] Guo H, Feng M, Song F, et al. Q-switched erbium-doped fiber laser based on silver nanoparticles as a saturable absorber. IEEE Photonics Technol Lett 2016;28:135–8.
[49] Ahmad H, Ruslan NE, Ali ZA, et al. Ag-nanoparticle as a Q switched device for tunable C-band fiber laser. Opt Commun 2016;381:85–90.
[50] Ahmad H, Samion MZ, Muhamad A, Sharbirin AS, Ismail MF. Passively Q-switched thulium-doped fiber laser with silver-nanoparticle film as the saturable absorber for operation at 2.0 μm. Laser Phys Lett 2016;13:126201.
[51] Yamashita S, Inoue Y, Maruyama S, et al. Saturable absorbers incorporating carbon nanotubes directly synthesized onto substrates and fibers and their application to mode-locked fiber lasers. Opt Lett 2004;29:1581–3.
[52] Fu B, Popa D, Zhao Z, et al. Wavelength tunable soliton rains in a nanotube-mode locked Tm-doped fiber laser. Appl Phys Lett 2018;113:193102.
[53] Bao Q, Zhang H, Wang Y, et al. Atomic-layer graphene as a saturable absorber for ultrafast pulsed lasers. Adv Funct Mater 2009;19:3077–83.
[54] Fu B, Hua Y, Xiao X, et al. Broadband graphene saturable absorber for pulsed fiber lasers at 1, 1.5, and 2 μm. IEEE J Sel Top Quantum Electron 2014;20:411–5.
[55] Fu B, Li J, Cao Z, Popa D. Bound states of solitons in a harmonic graphene-mode-locked fiber laser. Photonics Res 2019;7:116–20.
[56] Guo B, Xiao Q, Wang S, Zhang H. 2D layered materials: synthesis, nonlinear optical properties, and device applications. Laser Photonics Rev 2019;13:1800327.
[57] He J, Tao L, Zhang H, Zhou B, Li J. Emerging 2D materials beyond graphene for ultrashort pulse generation in fiber lasers. Nanoscale 2019;11:2577–93.
[58] Ma C, Wang C, Gao B, Adams J, Wu G, Zhang H. Recent progress in ultrafast lasers based on 2D materials as a saturable absorber. Appl Phys Rev 2019;6:041304.
[59] Fu B, Sun J, Wang G, et al. Solution-processed two-dimensional materials for ultrafast fiber lasers (invited). Nanophotonics 2020; DOI: 10.1515/nanoph-2019-0558.
[60] Jiang T, Yin K, Wang C, et al. Ultrafast fiber lasers mode-locked by two-dimensional materials: review and prospect. Photonics Res 2020;8:78–90.
[61] Compagnini G, Condorelli M, Fragalà ME, et al. Growth kinetics and sensing features of colloidal silver nanoplates. J Nanomater 2019;2019:7084731.
[62] Martinez A, Fuse K, Xu B, Yamashita S. Optical deposition of graphene and carbon nanotubes in a fiber ferrule for passive mode-locked lasing. Opt Express 2010;18:23054–61.
[63] Wang P, Hu D, Zhao K, Jiao L, Xiao X, Yang C. Dissipative rogue waves among noise-like pulses in a Tm fiber laser mode locked by a monolayer MoS_2 saturable absorber. J Sel Top Quantum Electron 2018;24:1800207.